

000 001 CYBERV: A CYBERNETIC FRAMEWORK FOR ENHANC- 002 003 004 005 006 007 008 009 010 011 012 013 014 015 016 017 018 019 020 021 022 023 024 025 026 027 028 029 030 031 032 033 034 035 036 037 038 039 040 041 042 043 044 045 046 047 048 049 050 051 052 053 CYBERV: A CYBERNETIC FRAMEWORK FOR ENHANC- ING LOGICAL REASONING IN VIDEO UNDERSTANDING

Anonymous authors

Paper under double-blind review

ABSTRACT

Current Multimodal Large Language Models (MLLMs) may struggle with tasks requiring deep logical reasoning about video content, primarily stemming from the feed-forward processing nature, which limits their ability for self-correction and iterative refinement. To address these limitations, we propose a novel framework inspired by cybernetic principles, redesigning video MLLMs as adaptive systems capable of self-monitoring, self-correction, and dynamic resource allocation during inference. Our approach, **CyberV**, introduces a cybernetic loop consisting of an MLLM Inference System, a Sensor, and a Controller. Specifically, the sensor monitors MLLM forward processes. It collects intermediate interpretations, such as attention drift, then the controller determines when and how to trigger self-correction and generate feedback to guide the next round. This test-time adaptive scaling framework enhances frozen MLLMs without requiring training or additional components. Experiments demonstrate significant improvements on complex reasoning benchmarks: CyberV boosts Qwen2.5-VL-7B by **8.3%** and InternVL3-8B by **5.5%** on VideoMMMU, surpassing the competitive proprietary model GPT-4o. When applied to Qwen2.5-VL-72B, it yields a **10.0%** improvement, achieving performance even comparable to human experts. Furthermore, on other reasoning-focused benchmarks, our method shows consistent gains of 4.6% on the multiple-choice question section of MMVU and 2.4% on MMR-V, highlighting its robustness in enhancing logical reasoning for video understanding. The code will be released to support further research.

1 INTRODUCTION

Understanding dynamic visual scenes in videos is a fundamental challenge, with applications ranging from autonomous driving to content analysis and human-robot interaction. Multimodal Large Language Models have recently emerged as a powerful paradigm, demonstrating impressive capabilities by integrating pre-trained large language models with visual encoders to process and reason about video content Wang et al. (2023a); Bai et al. (2023); Team et al. (2024); Zhang et al. (2024b); Fei et al. (2025). However, deploying these models effectively, particularly for tasks that demand deep, multi-step logical reasoning on video content, presents significant hurdles. Current MLLMs often struggle with the computational demands of processing extended video streams (test-time scaling), exhibit brittleness to variations or unexpected events in the input (lack of robustness), and are prone to generating inaccurate, inconsistent, or hallucinatory interpretations (limited accuracy) Zhang et al. (2024b); Li et al. (2024a); Fei et al. (2024); Hu et al. (2025a); Han et al. (2024). In particular, directly applying reflection prompts performs poorly in video understanding (Figure 1). Even state-of-the-art MLLMs struggle to scale their capabilities effectively. Moreover, simply using chain-of-thought prompting may also degrade the model’s perceptual abilities (Appendix A.2).

We argue that these limitations stem from the feed-forward processing pipeline inherent in current MLLM architectures. These models typically process videos in a single, often computationally intensive, pass, lacking dynamic adaptation, self-correction, or targeted analysis based on evolving understanding or specific task demands. This contrasts sharply with biological systems, which continuously use feedback to regulate behavior and adapt to complex environments.

To address this gap, we propose incorporating principles from cybernetics – the study of control, communication, and self-regulation in systems Wiener (1948); Ashby (1956) – into the design of

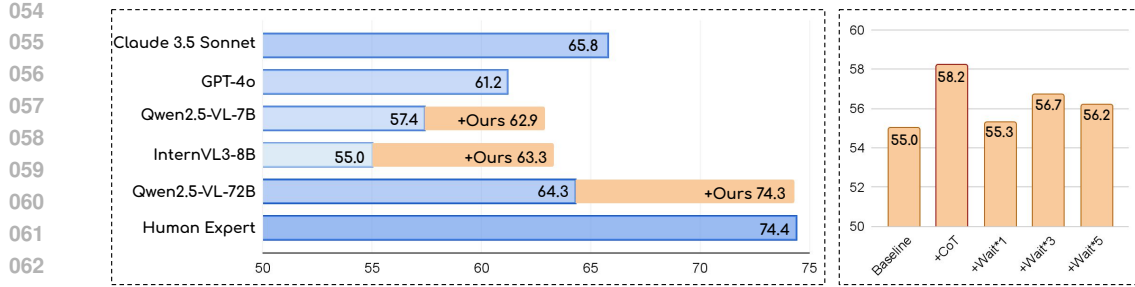


Figure 1: Performance on the VideoMMMU benchmark. **Left:** CyberV boosts small open-source models with only 7B parameters to outperform GPT-4o; with a larger model, CyberV surpasses the prior state-of-the-art and approaches the human level. **Right:** CoT reasoning improves results when using Qwen2.5-VL-7B, but multi-round reflection via “Wait” degrades performance.

MLLMs for video understanding. Cybernetics provides a rich theoretical framework centered on feedback loops, adaptive control, and goal-oriented behavior, enabling stable and effective operation in complex, dynamic settings. We hypothesize that by redesigning video MLLMs as cybernetic systems, capable of self-monitoring, self-correction, and adaptive resource allocation during inference, we can significantly enhance their performance.

Implementing these principles, we introduce **CyberV**, a framework structured as a dynamic feedback loop to create more robust and accurate MLLMs for video reasoning. The core of this cybernetic system consists of three components: the MLLM Inference System, the Sensor, and the Controller. Specifically, we generate responses by applying various scaling strategies within the MLLM inference system. These responses may come directly from the base MLLM model or be enhanced through techniques such as chain-of-thought prompting or the incorporation of key frames. The sensor monitors the inference processes and collects intermediate signals, such as the attention drift among different outputs and the prediction results, as evidence for the re-analysis of the controller. Given the evidence, the controller calculates the confidence score and determines whether to terminate the loop or to forcibly trigger a self-correction process to avoid unreliable responses during inference. If the termination condition is not met, the controller takes action by injecting the generated feedback into the MLLM’s input for the next round of inference, closing the entire cybernetic loop.

We demonstrate the efficacy of the proposed cybernetic mechanisms on challenging video understanding benchmarks that require complex reasoning. Our experiments demonstrate that CyberV can remarkably improve the performance of a relatively small model by a large margin. As shown in Figure 1, it improves the accuracy of Qwen2.5-VL-7B by 8.3% and InternVL3-8B by 5.5%, allowing both models to surpass GPT-4o on the VideoMMMU benchmark Hu et al. (2025b). Furthermore, when applied to a larger model, Qwen2.5-VL-72B, our approach yields a 10.0% improvement over the baseline, achieving performance comparable to human experts. To further validate its effectiveness, our method also delivers consistent improvements on other video reasoning benchmarks. For instance, based on the Qwen2.5-VL-7B model, it achieves gains of 4.6% on the multiple-choice question section of MMVU Zhao et al. (2025) and 2.4% on MMR-V Zhu et al. (2025b). Extensive ablation studies show the effectiveness of each component in our CyberV framework. Our **contributions** can be summarized as follows:

- We propose **CyberV**, a test-time adaptive scaling framework based on cybernetic feedback control that enhances the reasoning abilities of frozen MLLMs without training or extra components (vision expert models).
- We introduce an **attention-based** monitoring mechanism and an adaptive scoring controller that jointly govern strategy selection during inference.
- CyberV empowers small models to outperform proprietary systems like GPT-4o, and enables large open-source models to achieve state-of-the-art results on VideoMMMU. Extensive experiments demonstrate the effectiveness and robustness of our approach on **complex video reasoning tasks**.

108

2 RELATED WORK

109
 110 **Multi-modal Large Language Models in Video.** Multi-modal large language models (MLLMs)
 111 have seen growing attention in the video domain, with numerous video-specific models Zhang et al.
 112 (2024b; 2025a); Li et al. (2024d); Shu et al. (2024); Zhang et al. (2024a); Wang et al. (2025) and
 113 foundation models like the Qwen-VL Bai et al. (2023); Wang et al. (2024); Bai et al. (2025) and
 114 InternVL Chen et al. (2024c;a); Zhu et al. (2025a) series being developed. While these architectures
 115 demonstrate impressive perception capabilities, most struggle with complex reasoning over video
 116 content. To address this gap, recent efforts Guo et al. (2025a); Muennighoff et al. (2025); Shao
 117 et al. (2024) introduce reinforcement learning and test-time scaling strategies to enhance language
 118 model reasoning, and have been extended to video understanding through models such as Video-
 119 R1 Feng et al. (2025), VideoChat-R1 Li et al. (2025), and TinyLLaVA-Video-R1 Zhang et al. (2025b).
 120 In parallel, video chain-of-thought (CoT) prompting methods such as Video-of-Thought Fei et al.
 121 (2024), Chain-of-Shot Hu et al. (2025a), Logic-in-Frames Guo et al. (2025b) decompose complex
 122 video reasoning tasks into manageable sub-problems, addressing them step-by-step from low-level
 123 perception to high-level cognition. However, most existing approaches require supervised post-
 124 training or auxiliary models. In contrast, our work explores a training-free, single-model strategy that
 125 performs strongly on logic-based video tasks, suggesting that simple, modular inference techniques
 126 can yield robust multimodal reasoning.

127 **Test Time Scaling.** This direction Snell et al. (2024); Muennighoff et al. (2025); Liu et al. (2025) is a
 128 promising strategy for improving LLM performance by allocating more compute during inference.
 129 TTS methods generally fall into two categories: **Sequential Scaling**, which prolongs the reasoning
 130 process (e.g. chain of thought Wei et al. (2022), reflection Muennighoff et al. (2025)); and **Parallel
 131 Scaling**, which explores multiple reasoning paths and selects the best (e.g. Best-of-N Brown et al.
 132 (2024)). Parallel methods are often combined with sequential strategies to form complex search
 133 procedures, such as tree search Liu et al. (2025), with majority voting Wang et al. (2023b), output
 134 reward models (ORMs) Xin et al. (2024), and process reward models (PRMs) Uesato et al. (2022),
 135 often used to verify reasoning steps. While effective in textual tasks Muennighoff et al. (2025); Liu
 136 et al. (2025), TTS remains underexplored in video understanding. Our findings suggest that directly
 137 applying existing techniques often yields limited gains, highlighting the need for modality-aware
 scaling strategies.

138 **Cybernetics in Machine Learning and AI Systems.** Cybernetics, first formalized by Wiener Wiener
 139 (1948), provides a theoretical framework for self-regulating systems composed of three core compo-
 140 nents: a sensor for observing system states, a controller for decision-making, and a plant or system
 141 being controlled McCulloch & Pitts (1943). While influential in early AI research Ashby (1956);
 142 von Foerster (1952), its integration into modern deep learning remains limited. Some recent works
 143 have introduced feedback mechanisms into neural architectures Huang et al. (2020); Zhang & Lu
 144 (2023), but these often require architectural modifications or specialized training. In contrast, our
 145 approach utilizes the MLLM Inference System, Sensor, and Controller to apply cybernetic principles,
 146 significantly improving performance without the need for additional training.

147

3 METHOD

148

3.1 CYBERNETIC VIEW FOR VIDEO TEST-TIME SCALING

149 Test-time scaling for multimodal large language models (MLLMs), particularly in logic-based video
 150 understanding tasks, presents significant challenges. Unlike text-only reasoning, where techniques
 151 such as chain-of-thought and self-reflection prompting can be applied with moderate success, MLLMs
 152 face greater complexity due to the temporal, visual, and semantic richness of video data. Existing
 153 approaches Bai et al. (2025); Zhu et al. (2025a); Li et al. (2024a) apply static inference strategies
 154 that do not adapt to input difficulty, uncertainty, or reasoning failure, leading to inefficiencies and
 155 suboptimal performance. To overcome these limitations, we propose a cybernetic framework that
 156 transforms test-time inference into a feedback-driven, adaptive process inspired by the principles
 157 of control and regulation in cybernetics. We conceptualize video reasoning during inference as a
 158 closed-loop control system consisting of three interdependent components:

159 **MLLM Inference System:** This is the plant in the cybernetic loop, responsible for executing
 160 inference over multimodal input. Responses serve as raw material for further evaluation.

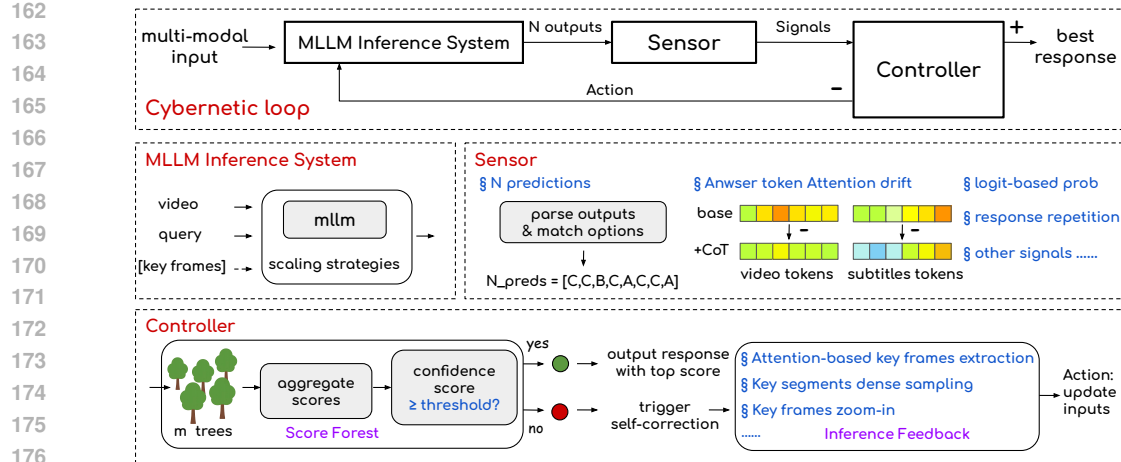


Figure 2: **Overall framework of CyberV.** CyberV models test-time video understanding as a closed-loop cybernetic process with three modules: **MLLM Inference System**, **Sensor**, and **Controller**. The inference system executes inference scaling strategies with a frozen MLLM, generating N outputs. The sensor monitors the MLLM forward process, extracting signals such as parsed prediction and attention drift. The controller uses a **Score Forest** to evaluate response reliability, triggering self-correction via the **Inference Feedback** module if confidence is low. The updated input is then used to re-invoke the MLLM. This feedback loop enables adaptive and robust test-time reasoning.

Sensor: The Sensor monitors the Inference System and extracts key signals such as predicted options and attention drift among different responses. These signals reflect the inference reliability, forming the basis for later decision-making.

Controller: The Controller is the central decision-making unit of the cybernetic system. It receives multiple signals from the Sensor, and evaluates the confidence of each candidate response using a rule-based scoring ensemble. Based on a thresholding policy, it decides whether to accept the output or trigger further inference with generated feedback.

Specifically, given a video V , a query q that includes the question and the video subtitles (if available), and a strategy set $\Pi = \{\pi_1, \dots, \pi_N\}$, the frozen model \mathcal{M} generates candidate responses $\{r_i\}_{i=1}^N$, where each r_i can be expressed as $r_i = \mathcal{M}_{\pi_i}(q, V)$. These responses are then passed back to the Sensor and Controller for evaluation, forming a closed feedback loop. This iterative process allows the model to monitor its interpretations, adjust inference paths in real time, and allocate computational resources more efficiently based on task relevance and video complexity. Unlike prior test time scaling approaches Muennighoff et al. (2025) that apply fixed reasoning templates regardless of context, our method dynamically modulates processing depth and focus, enhancing both accuracy and robustness.

As illustrated in Figure 2, the proposed framework **CyberV** implements this **cybernetic loop** to adaptively scale inference at test time without any parameter updates or supervision. It empowers a frozen model to handle diverse video understanding tasks by actively managing its reasoning process in response to control signals. The pseudo-code of CyberV is presented in Appendix A.3.

3.2 MLLM INFERENCE SYSTEM: EXECUTING TEST-TIME SCALING STRATEGIES

The MLLM inference system, the plant in our cybernetic loop, executes diverse test-time scaling strategies on multimodal input. We adopt the Best-of-N (BoN) scheme that executes N forward passes in parallel to generate a set of candidate responses. Each inference path may vary in its configuration, including direct answer using the base model, chain-of-thought prompting to encourage reasoning, such as “Thinking Process:”, or the incorporation of visually enhanced inputs such as injected key frames. This design enables the system to adaptively combine structured reasoning and perceptual reinforcement based on task uncertainty. Compared to more complex search strategies, such as performing tree search, Best-of-N offers a simpler yet effective alternative.

216 3.3 SENSOR: SIGNAL EXTRACTION FROM MLLM FORWARD PROCESSES
217218 The Sensor monitors the forward execution of the MLLM and extracts informative signals that serve
219 as the basis for confidence evaluation and feedback decisions.220 One key signal is the predicted answer label $\{\hat{y}_n\}_{n=1}^N$, obtained by parsing N textual responses
221 $\{r_n\}_{n=1}^N$, where $\hat{y}_n \in \mathcal{C}$, and \mathcal{C} is the candidate set of choices, e.g. A, B, C, D etc. The parsing relies
222 on explicit pattern matching.223 Additionally, the Sensor evaluates the model’s perceptual behavior by quantifying attention drift.
224 As the video and subtitles can be segmented according to the number of frames and timestamps,
225 we compare the attention distribution over these segments across two settings: a base response and
226 a chain-of-thought prompting variant. Specifically, the video is divided into K_1 segments and the
227 subtitles into K_2 segments. For each attention head $h \in \{1, \dots, H\}$, where H is the total number
228 of attention heads, we define the attention scores from the answer token to the video and subtitle
229 segments in the final layer as $\mathbf{A}_h^{\text{video}} \in [0, 1]^{1 \times K_1}$ and $\mathbf{A}_h^{\text{sub}} \in [0, 1]^{1 \times K_2}$. The attention drift signal
230 $\Delta^{\text{video}} \in [-1, 1]^{1 \times K_1}$ for video part and $\Delta^{\text{sub}} \in [-1, 1]^{1 \times K_2}$ for subtitles part is defined as:
231

232
$$\Delta^{\text{video}} = \frac{1}{H} \sum_{h=1}^H (\mathbf{A}_{h,\text{cot}}^{\text{video}} - \mathbf{A}_{h,\text{base}}^{\text{video}}), \quad \Delta^{\text{sub}} = \frac{1}{H} \sum_{h=1}^H (\mathbf{A}_{h,\text{cot}}^{\text{sub}} - \mathbf{A}_{h,\text{base}}^{\text{sub}}). \quad (1)$$

233

234 where the subscript “base” and “cot” refer to the base and chain-of-thought model responses, respectively.
235 The subtitle part is not considered when the video has no audio. We use the “base” response
236 as an anchor because its attention often reflects a more direct, foundational grounding on visual
237 evidence. Our goal is to diagnose whether the complex reasoning process induced by “cot” prompting
238 inadvertently causes the model’s focus to drift away from this crucial initial grounding. Therefore,
239 a large negative value of Δ on a certain segment indicates that the CoT process has significantly
240 distracted the model’s attention, suggesting degraded perceptual grounding. This mechanism is
241 designed to identify cases where the base model can answer correctly, but is misguided by the
242 CoT-induced reasoning path. The controller then uses this signal to trigger a self-correction via the
243 feedback loop.244 Beyond attention and answer prediction, the Sensor can also collect other forward-pass signals to
245 characterize response quality. For example, the softmax confidence of the predicted token, logit
246 stability across strategies, and repetition patterns in the response text. Together, these features offer
247 a rich diagnostic view of the model’s current inference behavior and serve as input to the control
248 mechanism that governs adaptive reasoning.
249250 3.4 CONTROLLER: DECISION MAKING AND FEEDBACK CONSTRUCTION
251252 The Controller governs the adaptive reasoning process by making two key decisions: whether the
253 current inference results are sufficiently reliable for output, and if not, how to generate actionable
254 feedback to revise the model’s input for the next iteration. It comprises two coordinated modules:
255 a **Score Forest** for response evaluation and an **Inference Feedback** module for corrective input
256 construction.257 **Score Forest: Confidence-Aware Evaluation and Thresholding.** Given N candidate responses
258 and multiple signals from the sensor, the Score Forest assigns each response a multi-dimensional
259 score vector $\mathbf{s}_n = (s_{n,1}, \dots, s_{n,m}) \in [0, 1]^m$, capturing semantic, probabilistic, and attention-related
260 qualities. Here, m is the number of trees in the forest, where each tree maps extracted signals to a
261 score via a distinct mechanism. In our implementation ($m = 5$), the rule-based scoring mechanisms
262 include: an **Attention Retention Score** from the attention drift signal Δ ; the raw **Answer Confidence**
263 **Score** based on softmax probability of the predicted answer token.; a binary **Confidence Stability**
264 **Score** to penalize significant drops after CoT; a **Relative Rank Score** formulated as $1 - (\text{rank}_n - 1)/N$
265 derived from confidence order; and a binary **Text Repetition Score** to penalize redundancy where a
266 long sequence is repeated beyond five times. The final score S_n for each response is computed as the
267 average of these individual scores: $S_n = \frac{1}{m} \sum_{i=1}^m s_{n,i}$.268 Furthermore, we can calculate the top-scoring option based on these scores. The score of the best
269 option, $\text{TopScore} \in [0, N]$, can be calculated by $\text{TopScore} = \max_{c \in \mathcal{C}} \sum_{n: \hat{y}_n = c} S_n$. If the top
score satisfies the confidence threshold, i.e., $\text{TopScore} \geq \tau \cdot N$, where the threshold $\tau \in [0, 1]$,

270 Table 1: **Performance on the VideoMMM benchmark (accuracy %).** The results are grouped by
 271 evaluation track (Perception, Comprehension, Adaptation) and academic discipline (Art, Business,
 272 Science, Medicine, Humanities, and Engineering). Yellow rows indicate open-source MLLMs, while
 273 blue rows indicate proprietary models. “*w/sub*” indicate our baselines with subtitle input.

| Model | Overall | Results by Track | | | Results by Discipline | | | | | |
|---|---------------------|------------------|-------------|-------------|-----------------------|-------------|-------------|-------------|-------------|-------------|
| | | Percep. | Compr. | Adapt. | Art. | Biz. | Sci. | Med. | Hum. | Eng. |
| Human Expert | 74.4 | 84.3 | 78.7 | 60.3 | 81.0 | 78.8 | 74.2 | 70.5 | 84.8 | 69.9 |
| LLaVA-OneVision-7B Li et al. (2024a) | 33.9 | 40.0 | 31.0 | 30.7 | 49.2 | 29.6 | 34.9 | 31.8 | 46.7 | 29.2 |
| VILA1.5-40B Lin et al. (2024) | 34.0 | 38.7 | 30.7 | 32.7 | 57.1 | 27.3 | 23.5 | 38.0 | 41.9 | 32.5 |
| LLaVA-Video-7B Zhang et al. (2024b) | 36.1 | 41.7 | 33.3 | 33.3 | 65.1 | 34.1 | 32.6 | 42.6 | 45.7 | 27.4 |
| InternVL2-8B Chen et al. (2024b) | 37.4 | 47.3 | 33.3 | 31.7 | 55.6 | 34.1 | 30.3 | 34.1 | 41.9 | 38.1 |
| LLaVA-OneVision-72B Li et al. (2024a) | 48.3 | 59.7 | 42.3 | 43.0 | 61.9 | 46.2 | 40.2 | 54.3 | 60.0 | 44.0 |
| LLaVA-Video-72B Zhang et al. (2024b) | 49.7 | 59.7 | 46.0 | 43.3 | 69.8 | 44.7 | 41.7 | 58.9 | 57.1 | 45.1 |
| Gemini 1.5 Flash Team et al. (2024) | 49.8 | 57.3 | 49.0 | 43.0 | 63.5 | 53.0 | 43.2 | 49.6 | 59.1 | 45.7 |
| Aria Li et al. (2024b) | 50.8 | 65.7 | 46.7 | 40.0 | 71.4 | 47.7 | 44.7 | 58.9 | 62.9 | 43.7 |
| Gemini 1.5 Pro Team et al. (2024) | 53.9 | 59.0 | 53.3 | 49.3 | 57.1 | 59.1 | 49.1 | 57.4 | 58.1 | 50.3 |
| Qwen2.5-VL-7B Bai et al. (2025) (w/ sub) | 55.0 | 72.7 | 53.7 | 38.7 | 73.0 | 56.1 | 46.2 | 58.1 | 73.3 | 47.8 |
| InternVL3-8B Zhu et al. (2025a) (w/ sub) | 57.4 | 77.0 | 49.7 | 45.7 | 61.9 | 59.1 | 53.0 | 60.5 | 74.3 | 51.3 |
| GPT-4o OpenAI (2024) | 61.2 | 66.0 | 62.0 | 55.7 | 69.5 | 66.9 | 51.6 | 64.8 | 69.5 | 57.1 |
| Qwen2.5-VL-72B Bai et al. (2025) (w/ sub) | 64.3 | 84.7 | 63.0 | 45.3 | 79.4 | 66.7 | 62.9 | 68.2 | 81.9 | 54.3 |
| Claude 3.5 Sonnet Anthropic (2024) | 65.8 | 72.0 | 69.7 | 55.7 | 66.7 | 75.0 | 56.1 | 58.1 | 75.2 | 66.1 |
| InternVL3-8B Zhu et al. (2025a) (+Ours) | 62.9 (+5.5) | 77.3 | 60.3 | 51.0 | 65.1 | 67.4 | 62.1 | 62.0 | 80.0 | 56.0 |
| Qwen2.5-VL-7B Bai et al. (2025) (+Ours) | 63.3 (+8.3) | 78.0 | 62.0 | 50.0 | 76.2 | 65.9 | 54.5 | 64.3 | 75.2 | 59.3 |
| Qwen2.5-VL-72B Bai et al. (2025) (+Ours) | 74.3 (+10.0) | 85.7 | 76.3 | 61.0 | 82.5 | 78.0 | 68.2 | 78.3 | 83.8 | 69.3 |

290
 291 the controller selects the top-score answer as the final output. Otherwise, the low confidence score
 292 indicates unreliable initial reasoning, and the controller triggers the Inference Feedback module to
 293 initiate a corrective update. Note that the widely used majority voting policy can be viewed as a
 294 special case of the Score Forest, where the score $S_n = 1$ for each response n and the threshold $\tau = 0$.
 295

296 **Inference Feedback: Visual Correction for Self-Revision.** When confidence is insufficient, the
 297 Controller invokes the Inference Feedback module to construct enhanced input that guides the next
 298 round of reasoning. This module identifies the top- k visual and subtitle segments that exhibit the
 299 greatest decrease in attention. Specifically, we define: $\mathcal{I}_{\text{video}} \subseteq \{1, \dots, K_1\}$ and $\mathcal{I}_{\text{sub}} \subseteq \{1, \dots, K_2\}$,
 300 where each set contains the indices of the top- k segments with the largest attention decrease:

$$\mathcal{I}_{\text{video}} = \text{TopK-Indices}(-\Delta_j^{\text{video}}), \quad \mathcal{I}_{\text{sub}} = \text{TopK-Indices}(-\Delta_j^{\text{sub}}). \quad (2)$$

301 For $\mathcal{I}_{\text{video}}$, we can directly extract the corresponding frames through the indices. For \mathcal{I}_{sub} , we trace
 302 their timestamps to locate the aligned frames. The union of these yields the final set of key frames.
 303 To restore the model’s degraded attention due to reasoning steps, the identified key frames can be
 304 seamlessly re-integrated into the original input sequence.

305 To further refine the model’s focus, we also support more visual content enhancement methods. Temporally, we perform dense sampling around selected key frames while sparsely sampling elsewhere.
 306 Spatially, we apply a zoom-in to emphasize evidence-rich regions by computing region-question
 307 relevance. To achieve this, key frames are partitioned into a grid of regions at multiple granularities.
 308 We then calculate the CLIP-based similarity between the question and each region, and the region
 309 with the highest relevance is cropped and used as an enhanced visual input. These enhanced inputs
 310 are then sent back to the MLLM inference system, enabling the model to refocus on critical evidence.
 311

312 4 EXPERIMENTS

313 **Benchmarks.** To rigorously evaluate our framework’s ability to enhance logical reasoning in video
 314 understanding tasks, we conduct experiments on three related benchmarks. **VideoMMM** Hu et al.
 315 (2025b) consists of 300 expert-level educational videos and 900 questions spanning six academic
 316 disciplines, making it the ideal testbed for an in-depth evaluation of our framework’s performance on
 317 knowledge-intensive reasoning. **MMVU** Zhao et al. (2025) tests expert-level reasoning with 1,000
 318 questions (validation set) on professional videos from 27 sub-disciplines, requiring the application of
 319 deep domain knowledge. **MMR-V** Zhu et al. (2025b) measures deep deductive reasoning with 1,257
 320 multiple-choice questions on 317 diverse videos. It challenges models with long-range, multi-hop
 321

324
 325 Table 2: Performance on other video reasoning benchmarks
 326 (accuracy %). “Val” means validation set, “MCQ” means
 327 multi-choice, and “w/sub” means adding subtitles in the
 328 prompt. The base model is Qwen2.5-VL-7B.

| Model | MMVU (Val, MCQ) | | MMR-V (w/sub) | |
|-------|--------------------|-------------|---------------|--------------------|
| | Overall | Implicit | Explicit | Overall |
| Base | 62.1 | 42.4 | 26.4 | 38.3 |
| +Ours | 66.7 (+4.6) | 44.0 | 30.9 | 40.7 (+2.4) |

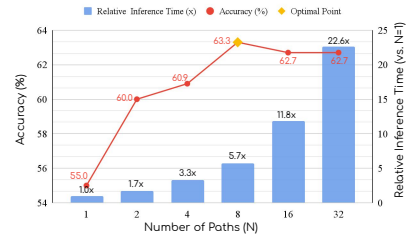
333
 334 logic to infer unstated information against confusing distractors. By evaluating on these benchmarks,
 335 we demonstrate our framework’s ability to enhance a spectrum of logical reasoning skills, from
 336 applying domain knowledge to performing deep deductions.

341 **Implementation Details.** We adopt Qwen2.5-VL Bai et al. (2025) and InternVL3 Zhu et al. (2025a)
 342 as the base models for all evaluations, using 64 uniformly sampled frames per video for Qwen2.5-VL
 343 and 32 frames for InternVL3. Subtitles, when needed, are extracted using Faster-Whisper Large-
 344 v3.¹. We adopt a two-round Best-of-N scheme across all benchmarks. In the Controller, response
 345 confidence is estimated via the Score Forest, and direct key frame injection is employed as the
 346 feedback mechanism. For all three benchmarks, we set $N = 8$ and $\tau = 0.3$ in the first round, using
 347 one base strategy and seven chain-of-thought (CoT) variants. In the second round, we set $N = 1$ and
 348 $\tau = 0$. We use accuracy as the evaluation metric for all benchmarks. All experiments are conducted
 349 on 8 GPUs, each equipped with 80 GB of memory.

351 4.1 MAIN RESULTS

353 Table 1 shows the primary results of our method on the **VideoMMMU** Hu et al. (2025b) benchmark.
 354 We compare our approach against two major categories of models: (1) open-source MLLMs, and
 355 (2) proprietary models such as GPT-4o and Claude 3.5 Sonnet. Human expert performance is also
 356 provided for reference. Our results show that **CyberV consistently enhances model performance**
 357 across a range of model scales. When applied to Qwen2.5-VL-7B, it achieves a notable +8.3%
 358 improvement over the base model, surpassing GPT-4o by 2.1% and approaching Claude 3.5 Sonnet.
 359 On InternVL3-8B, it brings a +5.5% gain, outperforming GPT-4o by 1.7%. For Qwen2.5-VL-72B,
 360 CyberV further boosts performance by +10.0%, exceeding Claude 3.5 Sonnet by 8.5% and reaching
 361 accuracy on par with human experts. These results show that even smaller open-source models can
 362 outperform proprietary LLMs through effective cybernetic inference-time scaling. In addition to
 363 the overall accuracy, we observe that CyberV is especially effective on the **comprehension** and
 364 **application** tracks, where reasoning and knowledge transfer are essential. By discipline, the most
 365 significant gains occur in **business, science, medicine, and engineering**, indicating that our method
 366 is crucial for knowledge-intensive video reasoning tasks.

367 To further demonstrate the framework’s effectiveness, we present additional results on two other
 368 video reasoning benchmarks, MMVU Zhao et al. (2025) and MMR-V, as shown in Table 2. For
 369 these experiments, we use Qwen2.5-VL-7B as the base model. On **MMVU**, our method achieves a
 370 significant **+4.6%** improvement. Note that here we focus specifically on its multiple-choice question
 371 (MCQ) section, as our current rule-based Score Forest is designed to score responses from a discrete
 372 set of candidate answers, making it less suited for free-form questions. On **MMR-V**, CyberV delivers
 373 a solid **+2.4%** overall gain, with consistent improvements observed across both its explicit and
 374 implicit reasoning sub-tasks. These results confirm that our framework provides stable and effective
 375 performance enhancements across a variety of video reasoning challenges. Furthermore, the results
 376 and discussion of perception-heavy video understanding benchmarks are provided in Appendix A.2.



377
 378 **Figure 3: Analysis of Performance**
 379 **vs. Efficiency.** The optimal balance is
 380 achieved at $N=8$, which is highlighted.

¹<https://github.com/SYSTRAN/faster-whisper>

378 Table 3: **Ablation Study on MLLM Inference System and Sensor.** Accuracy (%) on VideoMMMU
 379 under different inference configurations and search schemes for MLLM inference system, and
 380 different sources of attention drift for Sensor.

| (a) Impact of different scaling strategies. | | (b) Comparison of more search schemes. “KF” means key frames. | | (c) Comparison of different sources of attention drift. | |
|---|--------------|---|---------|---|---------|
| Strategy | Acc (%) | Scheme | Acc (%) | Attn Source | Acc (%) |
| Base | 48.6 | Base (+CoT&KF) | 60.0 | Base (+CoT) | 58.2 |
| +Subtitles | 55.0 (+6.4) | +Best-of-N (Ours) | 63.3 | + Video-Part | 59.9 |
| +CoT | 58.2 (+9.6) | +Tree Search | 62.8 | + Subtitles-Part | 60.0 |
| +Key Frames | 60.0 (+11.4) | | | | |

390 Table 4: **Ablation Study on Sensor and Controller.** Accuracy
 391 (%) on VideoMMMU under different scoring policies and visual
 392 self-correction methods in Controller.

| (a) Scoring policies. We set N=8 in Majority Voting and Score Forest. | | (b) Visual self-correction methods. | |
|---|---------|-------------------------------------|---------|
| Scoring Method | Acc (%) | Method | Acc (%) |
| Base (+CoT) | 58.2 | Base (+CoT) | 58.2 |
| Majority Voting | 61.9 | + Key Frames | 60.0 |
| Score Forest (Ours) | 63.3 | + Dense Sampling | 60.3 |
| | | + Spatial Zoom-in | 60.7 |

4.2 ABLATION STUDY ON MLLM INFERENCE SYSTEM AND SENSOR.

We conduct ablation studies on the VideoMMMU benchmark using Qwen2.5-VL-7B to investigate the contribution of each component in the CyberV framework.

Performance boost via multiple inference strategies. As shown in Table 3a, combining inference strategies like subtitles (+6.4%) and CoT prompting (+9.6%) significantly boosts performance. However, excessive reasoning may introduce distraction and attention drift. Our cybernetic loop alleviates this by incorporating attention-guided key frames, further improving accuracy to 60.0%. Note that here we adopt the **simplest form** of our framework: one base and one CoT response in the first round, followed by one response with key frames in the second round.

BoN outperforms complex search schemes. We justify our choice of Best-of-N (BoN), as it outperforms more complex strategies like PRM-guided tree search under a similar computational budget (Table 3b), confirming that BoN is a simpler yet more effective alternative for our framework.

Sensor benefits from different attention sources. The Sensor extracts intermediate signals like attention drift. As shown in Table 3c, incorporating subtitle-based attention drift alongside video-based drift offers a slight gain, indicating its complementary grounding value, though it may introduce noise when clear temporal anchors are absent.

4.3 ABLATION STUDY ON CONTROLLER.

Score Forest outperforms majority voting. We evaluate the Controller’s ability to make decisions based on uncertainty signals. Under the BoN (N=8) setting, our score forest, which aggregates multi-dimensional uncertainty, outperforms simple majority voting, as shown in Table 4a. These results confirm the critical role of the Controller in our cybernetic loop.

Different visual self-correction methods are effective. Beyond direct key frame injection, we analyze other visual self-correction methods. As shown in Table 4b, temporal dense sampling and spatial zoom-in further improve performance, with zoom-in achieving the best result at 60.7%. These results validate the effectiveness of multi-dimensional visual scaling in improving model focus and answer accuracy. Due to the additional complexity of these methods, we use direct key frames injection in the main experiments. More ablation studies are provided in Appendix A.1.

390 Table 5: **Stability analysis under different disturbance levels.** “+Ours” refers to the N=2
 391 setting.

| Setting | Base | +Ours |
|--------------------|------|-------|
| Uniform sampling | 55.0 | 60.0 |
| Disturb rate = 0.2 | 55.0 | 60.4 |
| Disturb rate = 0.4 | 55.4 | 60.2 |
| Disturb rate = 0.6 | 52.0 | 60.1 |

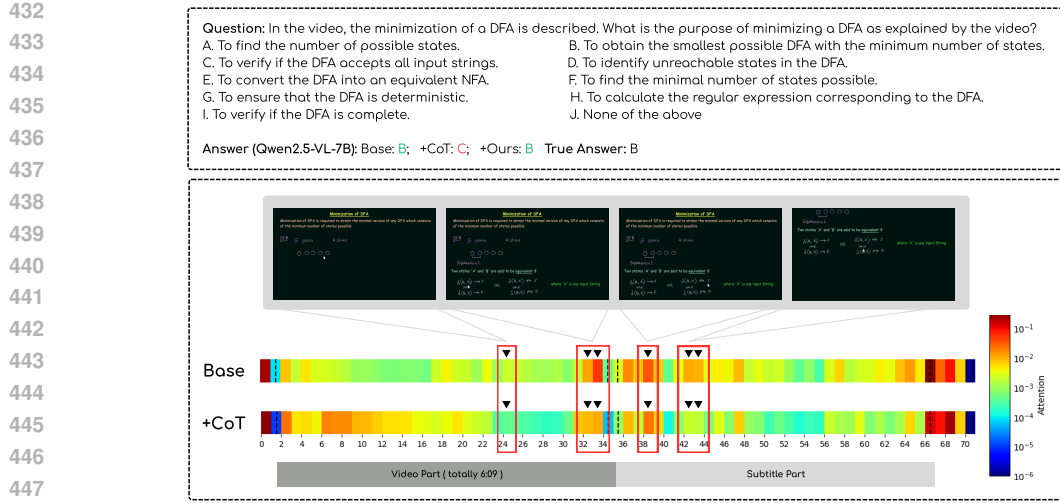


Figure 4: Attention map visualizations. Red boxes highlight segments where attention significantly drops after applying “CoT”. They may correspond to content that contains critical information. Under our control system, adding key frames after “CoT” helps rectify previously incorrect responses.

4.4 STABILITY ANALYSIS

To assess the robustness of our framework, we conduct a stability analysis inspired by control theory. We introduce temporal perturbations by replacing uniform frame sampling with a non-uniform variant, where each frame index is randomly shifted within a range determined by the disturb rate. As shown in Table 5, our method consistently outperforms the baseline across all disturbance levels, even as the baseline degrades. These results demonstrate that our method is stable and robust to non-uniform temporal distortions, confirming the strength of our cybernetic test-time scaling strategy in dynamically adapting to sampling perturbations while maintaining reliable performance.

4.5 ANALYSIS OF PERFORMANCE VS. EFFICIENCY

To find an optimal balance between performance and cost of our framework, we analyzed the trade-off by varying the number of inference paths (N). As shown in Figure 3, accuracy peaks at 63.3% for N=8, while inference time grows sub-linearly due to fixed overheads like data preprocessing. Since increasing N beyond this point yields diminishing returns at a prohibitive computational cost, our analysis confirms that N=8 provides the best trade-off, which is adopted in our main experiments.

4.6 VISUALIZATION

Figure 4 illustrates the effectiveness of our control system in identifying forgotten yet critical visual information via attention difference after CoT. By reintegrating these cues, the system corrects CoT-induced errors, demonstrating the effectiveness of CyberV in boosting reasoning while preserving perception. More visualizations and limitations are provided in Appendix A.4 and A.5.

5 CONCLUSION

We propose CyberV, a training-free, extra-model-free, test-time adaptive scaling framework designed to enhance logical reasoning in video understanding with multimodal large language models (MLLMs). Inspired by cybernetic principles, CyberV integrates a closed-loop architecture with a MLLM Inference System-Controller-Actuator design to monitor attention shifts, evaluate prediction uncertainty, and dynamically execute self-correction strategies. Extensive experiments across diverse benchmarks demonstrate the effectiveness of CyberV, achieving substantial gains on tasks requiring both deep knowledge application and complex deductive reasoning. Future work will explore more effective and efficient strategies to further improve complex multimodal reasoning.

486 ETHICS STATEMENT
487488 This work follows the ICLR Code of Ethics. All datasets used in our experiments, including
489 VideoMMMU, MMVU, MMR-V, VideoMME, WorldSense and MVBench, are publicly available
490 benchmarks. No private or sensitive information is involved, and the data usage strictly follows the
491 intended academic licenses.
492493 REPRODUCIBILITY STATEMENT
494495 We provide detailed descriptions of the model architectures, inference strategies, and hyperparameter
496 settings in the main paper and appendix. All datasets are public, and we will release our code to
497 ensure full reproducibility.
498499 LLM USAGE STATEMENT
500501 Large language models (LLMs) are only used to polish the writing of this paper, including grammar
502 correction, phrasing, and improving clarity of exposition. They do not contribute to research ideation,
503 experimental design, data analysis, or the generation of results. All technical contributions and
504 findings are entirely due to the authors.
505506 REFERENCES
507508 Anthropic. Claude Team. Introducing Claude 3.5 Sonnet. [https://www.anthropic.com/](https://www.anthropic.com/clause/sonnet)
509 clause/sonnet, 2024.
510511 William Ross Ashby. An introduction to cybernetics. 1956.
512513 Jinze Bai, Shuai Bai, Yunfei Chu, Zeyu Cui, Kai Dang, Xiaodong Deng, Yang Fan, Wenbin Ge,
514 Yu Han, Fei Huang, et al. Qwen technical report. *arXiv preprint arXiv:2309.16609*, 2023.
515516 Shuai Bai, Keqin Chen, Xuejing Liu, Jialin Wang, Wenbin Ge, Sibo Song, Kai Dang, Peng Wang,
517 Shijie Wang, Jun Tang, et al. Qwen2. 5-vl technical report. *arXiv preprint arXiv:2502.13923*,
518 2025.
519520 Bradley Brown, Jordan Juravsky, Ryan Ehrlich, Ronald Clark, Quoc V Le, Christopher Ré, and
521 Azalia Mirhoseini. Large language monkeys: Scaling inference compute with repeated sampling.
522 *arXiv preprint arXiv:2407.21787*, 2024.
523524 Zhe Chen, Weiyun Wang, Yue Cao, Yangzhou Liu, Zhangwei Gao, Erfei Cui, Jinguo Zhu, Shenglong
525 Ye, Hao Tian, Zhaoyang Liu, et al. Expanding performance boundaries of open-source multimodal
526 models with model, data, and test-time scaling. *arXiv preprint arXiv:2412.05271*, 2024a.
527528 Zhe Chen, Weiyun Wang, Hao Tian, Shenglong Ye, Zhangwei Gao, Erfei Cui, Wenwen Tong, Kongzhi
529 Hu, Jiapeng Luo, Zheng Ma, et al. How far are we to gpt-4v? closing the gap to commercial
530 multimodal models with open-source suites. *Science China Information Sciences*, 67(12):220101,
531 2024b.
532533 Zhe Chen, Jiannan Wu, Wenhui Wang, Weijie Su, Guo Chen, Sen Xing, Muyan Zhong, Qinglong
534 Zhang, Xizhou Zhu, Lewei Lu, et al. Internvl: Scaling up vision foundation models and aligning
535 for generic visual-linguistic tasks. In *Proceedings of the IEEE/CVF conference on computer vision*
536 and pattern recognition, pp. 24185–24198, 2024c.
537538 Hao Fei, Shengqiong Wu, Wei Ji, Hanwang Zhang, Meishan Zhang, Mong Li Lee, and Wynne
539 Hsu. Video-of-thought: step-by-step video reasoning from perception to cognition. In *ICML*, pp.
540 13109–13125, 2024.
541542 Hao Fei, Yuan Zhou, Juncheng Li, Xiangtai Li, Qingshan Xu, Bobo Li, Shengqiong Wu, Yaoting
543 Wang, Junbao Zhou, Jiahao Meng, et al. On path to multimodal generalist: General-level and
544 general-bench. *arXiv preprint arXiv:2505.04620*, 2025.
545

540 Kaituo Feng, Kaixiong Gong, Bohao Li, Zonghao Guo, Yibing Wang, Tianshuo Peng, Benyou
 541 Wang, and Xiangyu Yue. Video-r1: Reinforcing video reasoning in mllms. *arXiv preprint*
 542 *arXiv:2503.21776*, 2025.

543 Javier Ferrando, Oscar Obeso, Senthooran Rajamanoharan, and Neel Nanda. Do i know this entity?
 544 knowledge awareness and hallucinations in language models. *arXiv preprint arXiv:2411.14257*,
 545 2024.

546 Chaoyou Fu, Yuhang Dai, Yondong Luo, Lei Li, Shuhuai Ren, Renrui Zhang, Zihan Wang, Chenyu
 547 Zhou, Yunhang Shen, Mengdan Zhang, et al. Video-mme: The first-ever comprehensive evaluation
 548 benchmark of multi-modal llms in video analysis. In *CVPR*, 2025.

549 Daya Guo, Dejian Yang, Haowei Zhang, Junxiao Song, Ruoyu Zhang, Runxin Xu, Qihao Zhu,
 550 Shirong Ma, Peiyi Wang, Xiao Bi, et al. Deepseek-r1: Incentivizing reasoning capability in llms
 551 via reinforcement learning. *arXiv preprint arXiv:2501.12948*, 2025a.

552 Weiyu Guo, Ziyang Chen, Shaoguang Wang, Jianxiang He, Yijie Xu, Jinhui Ye, Ying Sun, and Hui
 553 Xiong. Logic-in-frames: Dynamic keyframe search via visual semantic-logical verification for
 554 long video understanding. *arXiv preprint arXiv:2503.13139*, 2025b.

555 Kai Han, Jianyuan Guo, Yehui Tang, Wei He, Enhua Wu, and Yunhe Wang. Free video-llm: Prompt-
 556 guided visual perception for efficient training-free video llms. *arXiv preprint arXiv:2410.10441*,
 557 2024.

558 Jack Hong, Shilin Yan, Jiayin Cai, Xiaolong Jiang, Yao Hu, and Weidi Xie. Worldsense: Evaluating
 559 real-world omnimodal understanding for multimodal llms. *arXiv preprint arXiv:2502.04326*, 2025.

560 Jian Hu, Zixu Cheng, Chenyang Si, Wei Li, and Shaogang Gong. Cos: Chain-of-shot prompting for
 561 long video understanding. *arXiv preprint arXiv:2502.06428*, 2025a.

562 Kairui Hu, Penghao Wu, Fanyi Pu, Wang Xiao, Yuanhan Zhang, Xiang Yue, Bo Li, and Ziwei Liu.
 563 Video-mmmu: Evaluating knowledge acquisition from multi-discipline professional videos. *arXiv*
 564 *preprint arXiv:2501.13826*, 2025b.

565 Yujia Huang, James Gornet, Sihui Dai, Zhiding Yu, Tan Nguyen, Doris Y. Tsao, and Anima Anandku-
 566 mar. Neural networks with recurrent generative feedback. [https://doi.org/10.48550/
 567 arXiv.2007.09200](https://doi.org/10.48550/arXiv.2007.09200), Jul 2020. First submitted on 17 Jul 2020, latest version 10 Nov 2020.

568 Bo Li, Yuanhan Zhang, Dong Guo, Renrui Zhang, Feng Li, Hao Zhang, Kaichen Zhang, Peiyuan
 569 Zhang, Yanwei Li, Ziwei Liu, et al. Llava-onevision: Easy visual task transfer. *arXiv preprint*
 570 *arXiv:2408.03326*, 2024a.

571 Dongxu Li, Yudong Liu, Haoning Wu, Yue Wang, Zhiqi Shen, Bowen Qu, Xinyao Niu, Fan Zhou,
 572 Chengen Huang, Yanpeng Li, et al. Aria: An open multimodal native mixture-of-experts model.
 573 *arXiv preprint arXiv:2410.05993*, 2024b.

574 Kunchang Li, Yali Wang, Yinan He, Yizhuo Li, Yi Wang, Yi Liu, Zun Wang, Jilan Xu, Guo Chen,
 575 Ping Luo, et al. Mvbench: A comprehensive multi-modal video understanding benchmark. In
 576 *Proceedings of the IEEE/CVF Conference on Computer Vision and Pattern Recognition*, pp.
 577 22195–22206, 2024c.

578 Kunchang Li, Yali Wang, Yinan He, Yizhuo Li, Yi Wang, Yi Liu, Zun Wang, Jilan Xu, Guo Chen,
 579 Ping Luo, et al. Mvbench: A comprehensive multi-modal video understanding benchmark. In
 580 *CVPR*, pp. 22195–22206, 2024d.

581 Xinhao Li, Ziang Yan, Desen Meng, Lu Dong, Xiangyu Zeng, Yinan He, Yali Wang, Yu Qiao,
 582 Yi Wang, and Limin Wang. Videochat-r1: Enhancing spatio-temporal perception via reinforcement
 583 fine-tuning. *arXiv preprint arXiv:2504.06958*, 2025.

584 Ji Lin, Hongxu Yin, Wei Ping, Pavlo Molchanov, Mohammad Shoeybi, and Song Han. Vila: On
 585 pre-training for visual language models. In *CVPR*, pp. 26689–26699, 2024.

594 Runze Liu, Junqi Gao, Jian Zhao, Kaiyan Zhang, Xiu Li, Biqing Qi, Wanli Ouyang, and Bowen
 595 Zhou. Can 1b llm surpass 405b llm? rethinking compute-optimal test-time scaling. *arXiv preprint*
 596 *arXiv:2502.06703*, 2025.

597 Warren S. McCulloch and Walter Pitts. A logical calculus of the ideas immanent in nervous activity.
 598 *The Bulletin of Mathematical Biophysics*, 5(4):115–133, December 1943. ISSN 0007-4985. doi:
 599 10.1007/BF02478259.

600 Niklas Muennighoff, Zitong Yang, Weijia Shi, Xiang Lisa Li, Li Fei-Fei, Hannaneh Hajishirzi, Luke
 601 Zettlemoyer, Percy Liang, Emmanuel Candès, and Tatsunori Hashimoto. s1: Simple test-time
 602 scaling. *arXiv preprint arXiv:2501.19393*, 2025.

603 OpenAI. Hello gpt4-o. <https://openai.com/index/hello-gpt-4o/>, 2024.

604 Zhihong Shao, Peiyi Wang, Qihao Zhu, Runxin Xu, Junxiao Song, Xiao Bi, Haowei Zhang,
 605 Mingchuan Zhang, YK Li, Y Wu, et al. Deepseekmath: Pushing the limits of mathematical
 606 reasoning in open language models. *arXiv preprint arXiv:2402.03300*, 2024.

607 Yan Shu, Zheng Liu, Peitian Zhang, Minghao Qin, Junjie Zhou, Zhengyang Liang, Tiejun Huang,
 608 and Bo Zhao. Video-xl: Extra-long vision language model for hour-scale video understanding.
 609 *arXiv preprint arXiv:2409.14485*, 2024.

610 Charlie Snell, Jaehoon Lee, Kelvin Xu, and Aviral Kumar. Scaling llm test-time compute optimally
 611 can be more effective than scaling model parameters. *arXiv preprint arXiv:2408.03314*, 2024.

612 Gemini Team, Petko Georgiev, Ving Ian Lei, Ryan Burnell, Libin Bai, Anmol Gulati, Garrett
 613 Tanzer, Damien Vincent, Zhufeng Pan, Shibo Wang, et al. Gemini 1.5: Unlocking multimodal
 614 understanding across millions of tokens of context. *arXiv preprint arXiv:2403.05530*, 2024.

615 Jonathan Uesato, Nate Kushman, Ramana Kumar, Francis Song, Noah Siegel, Lisa Wang, Antonia
 616 Creswell, Geoffrey Irving, and Irina Higgins. Solving math word problems with process-and
 617 outcome-based feedback. *arXiv preprint arXiv:2211.14275*, 2022.

618 Heinz von Foerster. Cybernetics: Circular causal and feedback mechanisms in biological and social
 619 systems. In *Transactions of the Seventh Conference*. Josiah Macy Jr. Foundation, 1952.

620 Peng Wang, Shuai Bai, Sinan Tan, Shijie Wang, Zhihao Fan, Jinze Bai, Keqin Chen, Xuejing Liu,
 621 Jialin Wang, Wenbin Ge, et al. Qwen2-vl: Enhancing vision-language model’s perception of the
 622 world at any resolution. *arXiv preprint arXiv:2409.12191*, 2024.

623 Wenhui Wang, Zhe Chen, Xiaokang Chen, Jiannan Wu, Xizhou Zhu, Gang Zeng, Ping Luo, Tong
 624 Lu, Jie Zhou, Yu Qiao, and Jifeng Dai. Visionllm: Large language model is also an open-ended
 625 decoder for vision-centric tasks. In *NeurIPS*, 2023a.

626 Xuezhi Wang, Jason Wei, Dale Schuurmans, Quoc V Le, Ed H Chi, Sharan Narang, Aakanksha
 627 Chowdhery, and Denny Zhou. Self-consistency improves chain of thought reasoning in language
 628 models. In *ICLR*, 2023b.

629 Yi Wang, Xinhao Li, Ziang Yan, Yinan He, Jiashuo Yu, Xiangyu Zeng, Chenting Wang, Changlian
 630 Ma, Haian Huang, Jianfei Gao, et al. Internvideo2. 5: Empowering video mllms with long and rich
 631 context modeling. *arXiv preprint arXiv:2501.12386*, 2025.

632 Jason Wei, Xuezhi Wang, Dale Schuurmans, Maarten Bosma, Fei Xia, Ed Chi, Quoc V Le, Denny
 633 Zhou, et al. Chain-of-thought prompting elicits reasoning in large language models. In *NeurIPS*,
 634 volume 35, pp. 24824–24837, 2022.

635 Norbert Wiener. *Cybernetics or Control and Communication in the Animal and the Machine*. MIT
 636 press, 1948.

637 Huajian Xin, Daya Guo, Zhihong Shao, Zhizhou Ren, Qihao Zhu, Bo Liu, Chong Ruan, Wenda Li,
 638 and Xiaodan Liang. Deepseek-prover: Advancing theorem proving in llms through large-scale
 639 synthetic data. *arXiv preprint arXiv:2405.14333*, 2024.

648 Boqiang Zhang, Kehan Li, Zesen Cheng, Zhiqiang Hu, Yuqian Yuan, Guanzheng Chen, Sicong Leng,
 649 Yuming Jiang, Hang Zhang, Xin Li, et al. Videollama 3: Frontier multimodal foundation models
 650 for image and video understanding. *arXiv preprint arXiv:2501.13106*, 2025a.

651

652 Peiyuan Zhang, Kaichen Zhang, Bo Li, Guangtao Zeng, Jingkang Yang, Yuanhan Zhang, Ziyue
 653 Wang, Haoran Tan, Chunyuan Li, and Ziwei Liu. Long context transfer from language to vision.
 654 *arXiv preprint arXiv:2406.16852*, 2024a.

655 Wanpeng Zhang and Zongqing Lu. Adarefiner: Refining decisions of language models with adaptive
 656 feedback. <https://doi.org/10.48550/arXiv.2309.17176>, Sep 2023. First submitted
 657 on 29 Sep 2023, last revised 3 May 2024.

658

659 Xingjian Zhang, Siwei Wen, Wenjun Wu, and Lei Huang. Tinyllava-video-r1: Towards smaller lmms
 660 for video reasoning. *arXiv preprint arXiv:2504.09641*, 2025b.

661

662 Yuanhan Zhang, Jinming Wu, Wei Li, Bo Li, Zejun Ma, Ziwei Liu, and Chunyuan Li. Video
 663 instruction tuning with synthetic data. *arXiv preprint arXiv:2410.02713*, 2024b.

664

665 Yilun Zhao, Haowei Zhang, Lujing Xie, Tongyan Hu, Guo Gan, Yitao Long, Zhiyuan Hu, Weiyuan
 666 Chen, Chuhan Li, Zhijian Xu, et al. Mmvu: Measuring expert-level multi-discipline video
 667 understanding. In *Proceedings of the Computer Vision and Pattern Recognition Conference*, pp.
 668 8475–8489, 2025.

669

670 Jinguo Zhu, Weiyun Wang, Zhe Chen, Zhaoyang Liu, Shenglong Ye, Lixin Gu, Yuchen Duan, Hao
 671 Tian, Weijie Su, Jie Shao, et al. Internvl3: Exploring advanced training and test-time recipes for
 672 open-source multimodal models. *arXiv preprint arXiv:2504.10479*, 2025a.

673

674 Kejian Zhu, Zhuoran Jin, Hongbang Yuan, Jiachun Li, Shangqing Tu, Pengfei Cao, Yubo Chen, Kang
 675 Liu, and Jun Zhao. Mmr-v: What's left unsaid? a benchmark for multimodal deep reasoning in
 676 videos. *arXiv preprint arXiv:2506.04141*, 2025b.

677

678

679

680

681

682

683

684

685

686

687

688

689

690

691

692

693

694

695

696

697

698

699

700

701

702 **A APPENDIX**

703

704 **Overview.** In this appendix, we first provide more ablation studies on several component designs
 705 in A.1. Then, we discuss the results on perception-heavy benchmarks in A.2. Next, we include the
 706 PyTorch-style pseudo-code of our algorithm in A.3 to offer a clearer understanding of the overall
 707 inference process. After that, we present more visualization results in A.4. Finally, we discuss the
 708 limitations and future work in A.5.

709

710 **A.1 MORE ABLATIONS STUDIES**

711

712 **Ablation on scoring mechanism in Score Forest.**

713 In our Score Forest implementation, the number of trees (m) is set to 5. The five scoring mechanisms
 714 are Attention Retention Score, Answer Confidence Score, Confidence Stability Score, Relative Rank
 715 Score and Text Repetition Score. Details of the five scores have been introduced in the main paper.
 716 According to Table 6, we conduct an ablation study on these five scores. Under a fixed random seed
 717 setting, the experiments demonstrate the effectiveness of each scoring mechanism, as removing any
 718 single one results in a drop in overall performance.

719 **Ablation study on attention extraction from different layers.** Recent studies in model interpretability
 720 suggest that the final layers of large language models tend to capture more high-level semantic
 721 information that directly contributes to the model’s output decisions Ferrando et al. (2024). Motivated
 722 by this, we evaluate the effectiveness of extracting attention signals from different depths of the
 723 LLM component in Qwen2.5-VL-7B, which contains 28 transformer layers in total. Specifically, we
 724 experiment with extracting attention maps from the last 1, 4, and 7 layers, and report the results in
 725 Table 7. Extracting attention solely from the final layer yields an accuracy of 60.0%. Including the
 726 last 4 layers slightly reduces performance to 59.4%, while using the last 7 layers gives a marginal
 727 improvement to 60.2%. Overall, incorporating more layers introduces minor fluctuations, but yields
 728 consistent improvement over the baseline. For simplicity and computational efficiency, we finally
 729 extract attention only from the last layer in all experiments.

730 Table 6: Ablation study on the components of
 731 the Score Forest in our implementation. “w/o”
 732 stands for “without”.

| 734 Scoring Method | 735 Accuracy (%) |
|------------------------------|-------------------------|
| 736 Score Forest Baselines | 63.3 |
| 737 w/o Attention Retention | 63.2 |
| 738 w/o Answer Confidence | 62.7 |
| 739 w/o Confidence Stability | 62.6 |
| 740 w/o Relative Rank | 63.2 |
| 741 w/o Text Repetition | 62.9 |

730 Table 7: Attention extraction from different lay-
 731 ers. Here, we use Qwen2.5-VL-7B and compare
 732 the last 1st, 4th, and 7th layers.

| 734 Attention from | 735 Accuracy (%) |
|---------------------------|-------------------------|
| 736 Base (No key frame) | 58.2 |
| 737 Last 1 layer | 60.0 |
| 738 Last 4 layers | 59.4 |
| 739 Last 7 layers | 60.2 |

743 **A.2 PERFORMANCE ON PERCEPTION-HEAVY QUESTION-ANSWERING BENCHMARKS**

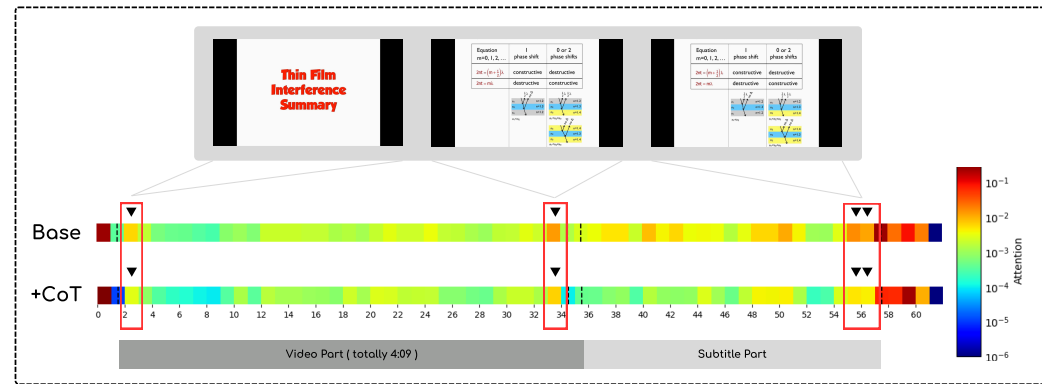
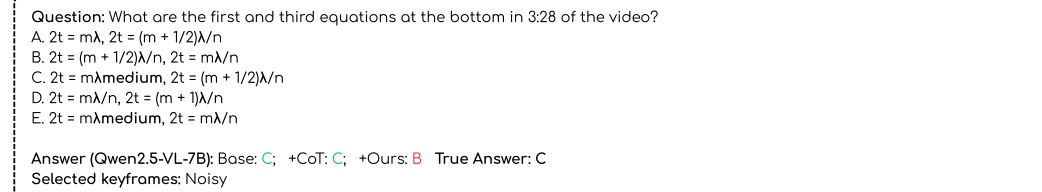
744

745 Both strong perceptual abilities and logical deduction are essential for accomplishing complex
 746 video understanding tasks. However, while test-time scaling methods are intended to guide model
 747 reasoning, we find that **simple chain-of-thought (CoT) prompting may impair a model’s direct**
 748 **perceptual capabilities.** We conduct tests on VideoMME Fu et al. (2025), WorldSense Hong et al.
 749 (2025), and MVBench Li et al. (2024c), three video understanding benchmarks where questions are
 750 predominantly focused on direct perception. As shown in Table 8, applying a simple CoT prompt
 751 significantly degraded the base model’s performance across all three benchmarks, with drops of
 752 -2.3%, -2.1%, and -4.6%, respectively. This suggests that **perception and reasoning do not trivially**
 753 **enhance one another**; in fact, an unguided reasoning process can inhibit foundational perceptual
 754 accuracy.

755 Our CyberV framework, however, is designed to mitigate this issue through its adaptive selection
 756 and control mechanisms. The controller adaptively selects the most reliable response and triggers

756 **Table 8: Performance on perception-heavy video understanding benchmarks (accuracy %).** The
 757 base model is Qwen2.5-VL-7B. Subtitles are added in VideoMME and WorldSense. Unlike “CoT”
 758 strategy, **CyberV maintains the base model’s perception performance.**

| Model | VideoMME | WorldSense | MVBench |
|-------|--------------------|--------------------|--------------------|
| Base | 70.5 | 46.0 | 66.7 |
| +CoT | 68.2 (-2.3) | 43.9 (-2.1) | 62.1 (-4.6) |
| +Ours | 71.6 (+1.1) | 47.1 (+1.1) | 67.5 (+0.8) |



772 Figure 5: Without confidence-based filtering (Score Forest) in the Controller, high-confidence correct
 773 answers in the first round also need to trigger unnecessary key frames extraction, leading to errors
 774 in the second round due to noisy frames. In this case, although the question refers to 3:28 of a 4:09
 775 video, the selected key frames focus on the beginning and end, resulting in an incorrect revision.

776 self-correction when necessary. As a result, unlike the fixed CoT approach, **our method avoids**
 777 **weakening the model’s perceptual abilities** and even yields slight performance gains of +1.1%
 778 on VideoMME, +1.1% on WorldSense, and +0.8% on MVBench. These outcomes underscore the
 779 necessity and utility of incorporating a self-correction mechanism. Along with results in the main
 780 paper, these findings demonstrate that CyberV can enhance a model’s logical reasoning capabilities
 781 while preserving its foundational perceptual skills, thereby enabling more complex video question-
 782 answering tasks.

A.3 PSEUDO-CODE OF CYBERV

783 Figure 8 illustrates the PyTorch-style pseudo-code of the CyberV architecture, which models video
 784 reasoning as a closed-loop control process. It consists of three core modules: the MLLM Inference
 785 System executes various scaling strategies; the Sensor monitors intermediate outputs and extracts
 786 key signals such as predictions and attention drift; and the Controller evaluates response reliability
 787 and, if needed, constructs feedback (e.g., key frames augmentation) to trigger self-correction. These
 788 components interact iteratively to improve reasoning quality without additional training.

A.4 MORE VISUALIZATION RESULTS

789 **More attention map visualizations.** In the main paper, we show that incorporating attention-guided
 790 key frames into the second-round inference can effectively correct CoT-induced errors, particularly in

810 cases where the base model initially produces the correct answer but CoT leads to an incorrect one.
 811 This demonstrates the utility of the cybernetic feedback loop in mitigating reasoning drift.
 812

813 However, as illustrated in Figure 5, applying visual self-correction indiscriminately (without
 814 confidence-based filtering) can introduce new errors. In this example, both the base model and
 815 CoT initially provide the correct answer with high confidence, yet the second round reversed the
 816 decision due to the influence of noisy and irrelevant key frames. The contrast between this failure
 817 case and successful examples underscores the importance of incorporating confidence-aware
 818 control to selectively trigger feedback only when necessary, thereby enhancing overall robustness and
 819 preserving performance on easy cases.

820 **Case studies on MMR-V.** We conduct visualization studies on the MMR-V benchmark to qualita-
 821 tively evaluate the effectiveness of our model. As depicted in Figures 6 and 7, these case studies
 822 illustrate both the strengths and limitations of the proposed cybernetic loop.

823 In Figure 6, a scenario is presented where both the base model and the Chain-of-Thought (CoT)
 824 approach fail, but our proposed method succeeds in comprehending the nuanced context of a video.
 825 Our method effectively leverages selected key frames that encapsulate the critical events, enabling it
 826 to deduce the correct, more complex situation: visiting a seriously ill boyfriend to wish him well.
 827 This case highlights our method’s strength in identifying and focusing on the most relevant temporal
 828 segments of a video to overcome misleading information from “CoT” and achieve accurate reasoning.

829 Figure 7 demonstrates a failure case where the performance of our model is degraded by noisy or
 830 irrelevant frames. This case shows a limitation of our method: inaccurate key frames extraction may,
 831 in certain instances, hinder the effectiveness of second-round visual enhancement, thereby failing to
 832 support meaningful self-correction.

833 A.5 LIMITATIONS AND FUTURE WORK DISCUSSION

834 While CyberV demonstrates notable improvements in test-time video reasoning, several limitations
 835 remain. First, the current key frames extraction relies on attention drift over video and subtitle
 836 segments. Although some critical frames are often covered, this approach may **introduce noisy or**
 837 **irrelevant frames**. Our cybernetic loop can mitigate their impact through selective correction, but
 838 more principled methods for noise filtering, temporal search and the utilization of signals remain
 839 important directions for future work. Second, **current state-of-the-art MLLMs exhibit limited**
 840 **capacity for temporally grounded perception and reasoning**. That is, the ability to precisely align
 841 and integrate the information from visual frames, subtitles, and questions along the temporal axis
 842 during the reasoning process. We believe that combining CyberV with future MLLMs possessing
 843 stronger multi-modal spatio-temporal understanding capabilities may yield greater benefits. Another
 844 limitation lies in **inference efficiency**. As the number of inference paths (N) and iterations increases,
 845 test-time latency grows manyfold. Developing more efficient implementations of the cybernetic loop,
 846 potentially via strategy pruning, presents another valuable avenue for future research.

847 Overall, while CyberV opens up a novel perspective on test-time adaptive reasoning, its full potential
 848 can be further unlocked through improvements in both base model capability and control system
 849 efficiency.

850
 851
 852
 853
 854
 855
 856
 857
 858
 859
 860
 861
 862
 863

864

865

866

867

868

869

870

871

872

873

874

875

876

877

878

879

880

881

882

883

884

885

886

887

888

889

890

891

892

893

894

895

896

897

898

899

900

901

902

903

904

905

906

907

908

909

910

911

912

913

914

915

916

917

Good Case:**CyberV boosts model performance****Benchmark:****MMR-V****Question:** What might the girl be writing a greeting card for?

- A. Valentine's Day celebration.
- B. Milo's birthday.
- C. A graduation celebration.
- D. Apology for a mistake.
- E. Milo's wedding anniversary.
- F. A heartfelt reunion with Milo.
- G. A thank you for help with a project.
- H. Christmas holiday greeting.
- I. A shared achievement celebration.
- J. To visit her seriously ill boyfriend and wish him well.
- K. A farewell for a move to a new city.

**Answer:** **J.****Qwen2.5-VL-7B:** **A.****Qwen2.5-VL-7B (+CoT):****Thinking process:**

1. The setting includes a bouquet of flowers, which often symbolize affection or care.
2. The girl is writing on a card, implying a personal message is being composed.
3. There is an envelope, suggesting this could be a message meant to be sent.
4. The mention of "for Milo" indicates the recipient of the message.

Final answer: **F.****Remark:** The key events were not accurately identified, leading the model to focus on misleading information such as "for Milo".**Qwen2.5-VL-7B (Ours):****Best-of-8 output:** **[A, B, F, J, B, B, F, F]**

Uncertain!

Selected keyframes:**Final answer:** **J.****Remark:** The selected keyframes cover the timestamps when the events mentioned in the question occur.

Figure 6: Base model and "CoT" fail to answer but our method performs well.

918

919

920

921

Bad Case:**Noisy frames may degrade model performance**

922

923

Benchmark:**MMR-V**

924

Question: What message does the entire video intend to convey?

- Having advanced abilities makes someone superior in all situations.
- Playing soccer requires extraordinary physical talent.
- People should fear what they don't understand.
- Strength always wins respect from others.
- Inclusion and acceptance can transcend differences, even across major divides like human and non-human.
- Team sports are the only way to bring people together.
- Distinguishing oneself through physical displays should be everyone's goal.
- This telecommunications company has a strong signal transmission capability.**
- Childhood friendship is only about sports.
- A mysterious figure is always a potential danger.
- Robots are better at physical activities than humans.



925

926

927

928

929

930

931

932

933

934

935

936

937

938

939

940

941

942

943

944

Answer: **H.**

945

946

947

948

949

Qwen2.5-VL-7B: D.

950

951

952

953

954

Qwen2.5-VL-7B (+CoT):

955

956

957

958

959

960

961

962

963

964

965

966

967

968

969

970

971

Thinking process:

- The video shows a group of children playing soccer, with one child performing an acrobatic kick that causes another child to fall off a balcony.

- The video ends with a logo for Ooredoo and a message promoting their brand.

Final answer: **H.****Qwen2.5-VL-7B (Ours):****Best-of-8 output:** [D, D, H, E, F, E, F, E]

Uncertain!

Selected keyframes:**Final answer:** **F.****Remark:** The selection of keyframes is not accurate, which may lead to incorrect final answer.

Figure 7: Noisy frames may degrade model performance.

972
973
974
975
976
977
978
979
980
981
982

Pseudo-code of the CyberV architecture.

```

983
984
985 # Core module: Sensor
986 # signal extraction from MLLM forward
987 # processes
988 class Sensor:
989     def monitor(outputs):
990         signals = []
991         signals.append(get_predictions(
992             outputs))
993         signals.append(get_attn_drift(
994             outputs))
995         ...
996         return signals
997
998 # Core module: Controller
999 # decision making and feedback construction
1000 class Controller:
1001     def score_forest(out, attn_drift):
1002         # cal score for each response
1003         # aggregate scores for each option
1004         return score_list
1005
1006     def inference_feedback(signals):
1007         # key frames extraction
1008         video_based_kfs, sub_based_kfs = ...
1009         kf = video_based_kfs |
1010             sub_based_kfs
1011         # visual cues enhancement
1012         # Here is an example: directly
1013         augment key frames
1014         action = ("Add key frames.", kf)
1015         return action
1016
1017     def decide(signals):
1018         scores = score_forest(signals)
1019         response = best_answer(scores)
1020         if is_confident(scores):
1021             return True, response, None
1022         else:
1023             action = inference_feedback(
1024                 signals)
1025             return False, response, action

```

```

# Core module: MLLM Inference System
# Executing Inference Strategies
class MLLMSystem:
    # an MLLM. For example, Qwen2.5-VL-7B
    self.model = ...
    def execute(inputs):
        outputs = []
        # Use BoN to get N responses
        for s in inputs['strategies']:
            out = self.model.forward(inputs,
s)
            outputs.append(out)
        return outputs

# Cybernetic loop for one inference round
def run_one_loop(inputs):
    # Step 1: Run MLLM with multiple
    # strategies
    out = MLLMSystem.execute(inputs)
    # Step 2: Monitor outputs to extract
    # signals
    signals = Sensor.monitor(out)
    # Step 3: Decide when & how to trigger
    # self-correction
    flag, response, action = Controller.
    decide(signals)
    return flag, response, action

# Closed-loop inference over multiple rounds
def cyber_v(inputs):
    max_rounds = ...
    round_now = 1
    while True:
        flag, response, action =
        run_one_loop(inputs)
        if flag or round_now == max_rounds:
            return response
        inputs = update(inputs, action)
        round_now += 1

```

Figure 8: Pseudo-code of the CyberV architecture. The MLLM Inference System, Sensor and Controller cooperate to form a closed-loop control cycle for test-time video understanding.

1016
1017
1018
1019
1020
1021
1022
1023
1024
1025